

An efficient Galerkin meshfree analysis of shear deformable cylindrical panels

Dongdong Wang*

Department of Civil Engineering, Xiamen University, Xiamen, Fujian, 361005, China

Youcai Wu

Karagozian & Case, 2550 N Hollywood Way, Suite 500, Burbank, CA 91505, USA

(Received January 30, 2008, Accepted July 8, 2008)

Abstract. A Galerkin meshfree method is presented for analyzing shear deformable cylindrical panels. Based upon the analogy between the cylindrical panel and the curved beam a pure bending mode for cylindrical panel is rationally constructed. The meshfree approximation employed herein is characterized by an enhanced moving least square or reproducing kernel basis function that can exactly represent the pure bending mode and thus meets the requirement of Kirchhoff mode reproducing condition. The variational form is discretized using the efficient stabilized conforming nodal integration with a smoothed nodal gradient based curvature. The resulting meshfree formulation satisfies the integration constraint for bending exactness. Moreover, it is shown here that the smoothed gradient preserves several desired properties which are valid for the standard gradient obtained by direct differentiation, such as partition of nullity and reproduction of a constant strain field. The efficacy of the proposed approach is demonstrated by two benchmark cylindrical panel examples.

Keywords: cylindrical panel; meshfree method; stabilized conforming nodal integration; smoothed nodal gradient.

1. Introduction

Galerkin meshfree methods based on the moving least square (MLS, [Lancaster and Salkauskas 1981, Belytschko *et al.* 1994]) or reproducing kernel (RK, [Liu *et al.* 1995, Chen *et al.* 1996]) approximation have essential advantages on stability and accuracy and thus have attracted noticeable research attention from the academia as well as industry (Belytschko *et al.* 1994, Liu *et al.* 1995, Chen *et al.* 1996, Krysl and Belytschko 1996, Li *et al.* 2000, Li and Liu 2004, Hallquist 2003). Nonetheless for Galerkin type of formulations the domain integration has to be carried out using certain ways, among them the Gauss quadrature rule is frequently employed. The non-polynomial feature of MLS/RK shape functions makes higher order quadratures necessary and therefore the domain integration becomes much more computationally intensive compared with its FEM

*Corresponding author, Email: ddwang@xmu.edu.cn

counterpart. The high CPU cost actually prevents the Galerkin meshfree methods from widespread practical applications with large models. Collocation of the Galerkin weak form directly at meshfree nodal points provides desired computational efficiency but suffers from spatial stability problem (Beissel and Belytschko 1996).

To accelerate the meshfree computation and overcome the stability issue associated with nodal integration as well, (Beissel and Belytschko 1996) introduced a stabilization term consisting of the residual of the equilibrium equation into the weak form. Employment of the extra set of stress points in the meshfree formulations provides another applicable way to improve the stability behavior. This method was first proposed by Dyka and Ingel (1995) in one dimension and was generalized to higher dimensions by Randles and Libersky (2000). Rabczuk *et al.* (2004) also investigated the stress point stabilization within the Galerkin meshfree environment. (Chen *et al.* 2001, 2002) took a different path to enhance the stability of nodal integration through the employment of a novel smoothed nodal gradient and the assumed strain method. The proposed smoothed gradient matrix was shown to meet the integration constraint for linear exactness in the Galerkin approximation. This approach is referred as the stabilized conforming nodal integration (SCNI, [Chen *et al.* 2001]) meshfree formulation. Thereafter the SCNI formulation was generalized to meet bending exactness and analyze shear deformable beam/plate/shell problems (Chen *et al.* 2004, Wang and Chen 2004, Wang *et al.* 2006, Wang and Chen 2006, Chen and Wang 2006). Recently it was also further adapted to solve thin plate problems where the shear deformation can be neglected (Wang 2006, Wang and Chen 2008). Good numerical performance has been observed for these SCNI-based meshfree formulations.

In this work we wish to develop an SCNI meshfree method with particular refer to the problem of shear deformable cylindrical panels. A pure bending mode for the cylindrical panel is constructed based on its counterpart for the curved beam (Wang and Chen 2006). Then according to the Kirchhoff Mode Reproducing Condition (KMRC), a meshfree basis function is deduced to exactly represent this pure bending deformation. Consequently a curvature smoothing operation is performed and a resulting SCNI formulation is set up which is capable of reproducing the pure bending solution under the Galerkin framework. It is also shown that the smoothed nodal gradient preserves some desired properties of the conventional nodal gradient obtained by direct differentiation, i.e., the salient partition of nullity.

The rest of this paper is outlined as follows. In Section 2 the preliminaries of a shear deformable cylindrical panel are summarized. The pure bending deformation with constant curvature and zero membrane and shear deformations is discussed in Section 3. Then in Section 4 the approximation of field variables using a special meshfree approximation is illustrated. The integration constraint, smoothed gradient and its properties, and the resulting SCNI formulation are presented in Section 5. In Section 6 the efficacy of the proposed method is demonstrated by two numerical examples. Finally conclusions are given in Section 7.

2. Basic equations of cylindrical panel

Consider a cylindrical panel or shell with a curvature radius R occupying a domain $\mathcal{B} = \overline{\Omega} \times [-h, h]/2$ as shown in Fig. 1, where $\overline{\Omega} \in \mathbb{R}^2$, $\overline{\Omega} = \Omega \cup \Gamma$, Ω and Γ represent the mid-surface and associated boundary of shell, h is the shell thickness. The panel geometry is described by a right hand coordinate system (x, s, z) with x and $s = R\theta$ being the axial and hoop coordinates on the shell

mid-surface and z as the radial coordinate measuring from the mid-surface. The panel's thickness/radius ratio (h/R) is assumed small compared to unity and is neglected in this formulation. Let $\hat{u}, \hat{v}, \hat{w}$ be the displacements at a generic field point (x, s, z) along these coordinate directions, in a first order shear deformation theory they are assumed to vary linearly over the shell thickness and can be expressed as follows:

$$\begin{aligned} \hat{u}(x, s, z) &= u(x, s) - z\beta_x(x, s) \\ \hat{v}(x, s, z) &= v(x, s) - z\beta_\theta(x, s) \\ \hat{w}(x, s, z) &= w(x, s) \end{aligned} \tag{1}$$

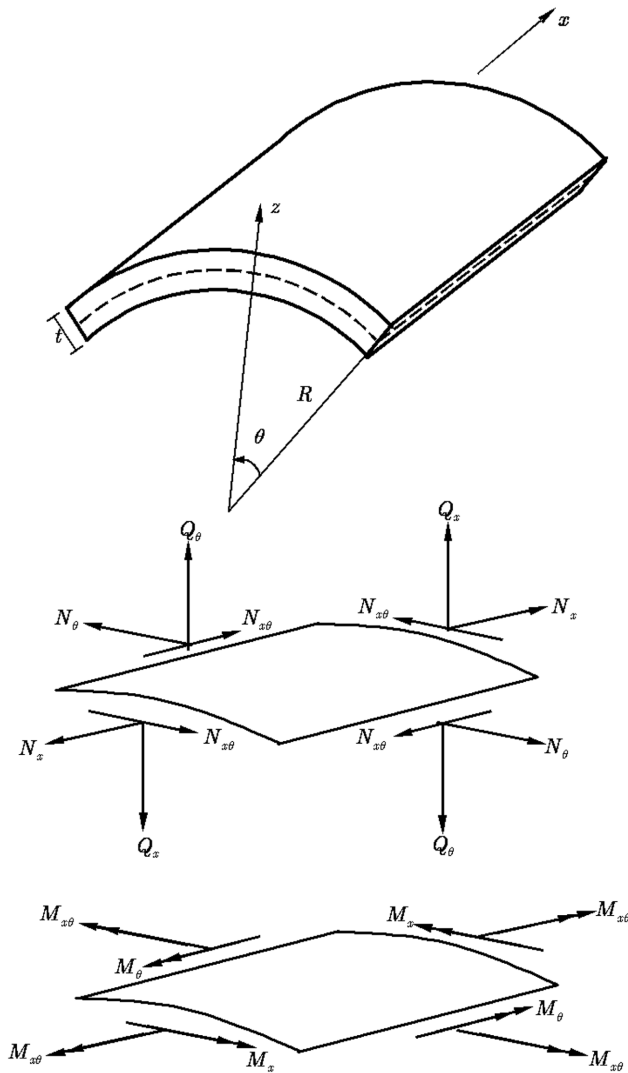


Fig. 1 Sign conventions for cylindrical panel

where (u, v, w) and (β_x, β_θ) denote the mid-surface displacements and two bending rotations at the location (x, s) , respectively. The other dependent field variables are the eight deformation measures $(\varepsilon_{xx}, \varepsilon_{\theta\theta}, \gamma_{x\theta}, \gamma_{xz}, \gamma_{\theta z}, \kappa_{xx}, \kappa_{\theta\theta}, \kappa_{x\theta})$, and their corresponding force and couple resultants $(N_x, N_\theta, N_{x\theta}, Q_x, Q_\theta, M_x, M_\theta, M_{x\theta})$. The sign conventions used in this study are also shown in Fig. 1.

For convenience of development, as shown below the strain measures are grouped into three parts, i.e., the in-plane membrane strain ε , the out-of-plane bending curvature κ and the shear strain γ . By substituting the displacement field of Eq. (1) into the standard displacement-strain relationship defined under the cylindrical coordinates (Timoshenko and Woinowsky-Krieger 1959), it can be found that these strains are related to the mid-surface displacements via:

$$\varepsilon = \begin{Bmatrix} \varepsilon_{xx} \\ \varepsilon_{\theta\theta} \\ \gamma_{x\theta} \end{Bmatrix} = \begin{Bmatrix} u_{,x} \\ v_{,s} + \frac{w}{R} \\ v_{,x} + u_{,s} \end{Bmatrix} \quad (2)$$

$$\kappa = \begin{Bmatrix} \kappa_{xx} \\ \kappa_{\theta\theta} \\ 2\kappa_{x\theta} \end{Bmatrix} = \begin{Bmatrix} \beta_{x,x} \\ \beta_{\theta,s} \\ \beta_{\theta,x} + \beta_{x,s} \end{Bmatrix} \quad (3)$$

$$\gamma = \begin{Bmatrix} \gamma_{xz} \\ \gamma_{\theta z} \end{Bmatrix} = \begin{Bmatrix} w_{,x} - \beta_x \\ w_{,s} - \frac{v}{R} - \beta_\theta \end{Bmatrix} \quad (4)$$

The constitutive equations linking the membrane force and moment resultants to their corresponding deformation measures for a linear elastic isotropic material are:

$$\mathbf{N} = \begin{Bmatrix} N_x \\ N_\theta \\ N_{x\theta} \end{Bmatrix} = \frac{Eh}{1-\nu^2} \begin{bmatrix} 1 & \nu & 0 \\ \nu & 1 & 0 \\ 0 & 0 & (1-\nu)/2 \end{bmatrix} \begin{Bmatrix} \varepsilon_{xx} \\ \varepsilon_{\theta\theta} \\ \gamma_{x\theta} \end{Bmatrix} = \mathbf{D}^m \varepsilon \quad (5)$$

$$\mathbf{M} = \begin{Bmatrix} M_x \\ M_\theta \\ M_{x\theta} \end{Bmatrix} = \frac{Eh^3}{12(1-\nu^2)} \begin{bmatrix} 1 & \nu & 0 \\ \nu & 1 & 0 \\ 0 & 0 & (1-\nu)/2 \end{bmatrix} \begin{Bmatrix} -\kappa_{xx} \\ -\kappa_{\theta\theta} \\ -2\kappa_{x\theta} \end{Bmatrix} = -\mathbf{D}^b \kappa \quad (6)$$

In addition the shear constitutive relations are given as:

$$\mathbf{Q} = \begin{Bmatrix} Q_x \\ Q_y \end{Bmatrix} = kh\mu \begin{bmatrix} 1 & 0 \\ 0 & 1 \end{bmatrix} \begin{Bmatrix} \gamma_{xz} \\ \gamma_{\theta z} \end{Bmatrix} = \mathbf{D}^s \gamma \quad (7)$$

where E , ν and μ are Young's modulus, Poisson's ratio, and shear modulus respectively, and $k = 5/6$ is the shear correction factor.

The five equilibrium equations of cylindrical panel are of the form:

$$\begin{cases} N_{xx,x} + N_{x\theta,s} + p_x = 0 \\ N_{x\theta,x} + N_{\theta\theta,s} + Q_\theta/R + p_\theta = 0 \\ Q_{x,x} + Q_{\theta,s} - N_{\theta\theta}/R + q = 0 \text{ in } \Omega \\ M_{xx,x} + M_{x\theta,s} - Q_x + m_x = 0 \\ M_{xy,x} + M_{\theta\theta,s} - Q_y + m_\theta = 0 \end{cases} \quad (8)$$

where $(p_x, p_\theta, q, m_x, m_\theta)$ are the applied tangential and normal tractions and moments. The equations in (8) are subjected to the following boundary conditions:

$$\begin{cases} u = \bar{u} \\ v = \bar{v} \\ w = \bar{w} \\ \beta_n = \bar{\beta}_n \\ \beta_t = \bar{\beta}_t \end{cases} \text{ on } \Gamma^{g_i} \quad \text{or} \quad \begin{cases} N_n = \bar{N}_n \\ N_t = \bar{N}_t \\ Q_n = \bar{Q}_n \\ M_{nn} = \bar{M}_{nn} \\ M_{nt} = \bar{M}_{nt} \end{cases} \text{ on } \Gamma^{h_i} \quad (9)$$

where the over-bar denotes a prescribed quantity, Γ^{g_i} and Γ^{h_i} represent the essential and natural parts of the boundary Γ with unit outward normal and tangential vectors \mathbf{n} and \mathbf{t} .

A variational statement of the equilibrium of Eq. (8) can be written as

$$\begin{aligned} \delta \Pi(\mathbf{u}) &= \int_{\Omega} \delta \boldsymbol{\varepsilon}^T \mathbf{D}^m \boldsymbol{\varepsilon} d\Omega + \int_{\Omega} \delta \boldsymbol{\kappa}^T \mathbf{D}^b \boldsymbol{\kappa} d\Omega + \int_{\Omega} \delta \boldsymbol{\gamma}^T \mathbf{D}^s \boldsymbol{\gamma} d\Omega \\ &\quad - \int_{\Omega} (\delta u p_x + \delta v p_y + \delta w q + \delta \beta_x m_x + \delta \beta_\theta m_y) d\Omega \\ &\quad - \int_{\Gamma^{h_i}} (\delta u \bar{N}_x + \delta v \bar{N}_\theta + \delta w \bar{Q}_n - \delta \beta_n \bar{M}_{nn} - \delta \beta_t \bar{M}_{nt}) d\Gamma = 0 \end{aligned} \quad (10)$$

where $\mathbf{u} = \{u, v, w, \beta_x, \beta_\theta\}^T$, and use is made of the constitutive equations from (5) to (7).

3. Pure bending mode

The purpose of discussing the pure bending mode here is that to alleviate the shear and membrane locking, a numerical approximation is expected not to produce parasitic shear and membrane deformations when representing a pure bending mode, as also known as the KMRC. So the pure bending mode can serve as a useful basis for constructing effective numerical schemes free of locking. This has been demonstrated in the previous works (Wang and Chen 2004, Wang and Chen 2006). However for a cylindrical panel it is not straightforward to find a general pure bending

solution. Rather than sticking to directly solve a pure bending solution, here we build a pure bending solution for cylindrical shell by generalizing the counterpart of curved beam, which was discussed in details in (Wang and Chen 2006). Based on the pure bending of curved beam, the displacement field of a bending mode for cylindrical panel can be written as:

$$\begin{cases} u = 0 \\ v = cR^2(\sin \theta - \theta) \\ w = cR^2(1 - \cos \theta) \\ \beta_x = 0 \\ \beta_\theta = cR\theta = cs \end{cases} \quad (11)$$

with c being an arbitrary constant.

Invoking the kinematics and constitutive relationships from Eqns. (2) to (7), the resulting deformation, force and couple fields of Eq. (11) are obtained as:

$$\begin{cases} \varepsilon_{xx} = 0; \varepsilon_{\theta\theta} = 0; \gamma_{x\theta} = 0 \\ \kappa_{xx} = 0; \kappa_{\theta\theta} = c; 2\kappa_{x\theta} = 0 \\ \gamma_{xz} = 0; \gamma_{\theta z} = 0 \end{cases} \quad (12)$$

$$\mathbf{M} = \begin{Bmatrix} M_x \\ M_\theta \\ M_{x\theta} \end{Bmatrix} = \frac{-Eh^3c}{12(1-\nu^2)} \begin{Bmatrix} \nu \\ 1 \\ 0 \end{Bmatrix} = \text{constant} \quad (13)$$

The constant curvatures and moments verify the displacement field defined in Eq. (11) corresponds to a pure bending mode of cylindrical panel. Thus it is desired that the employed approximation and discretized Galerkin meshfree equations can reproduce this mode exactly.

4. Meshfree approximation

4.1 MLS/RK shape function

The MLS/RK (Lancaster and Salkauskas 1981, Belytschko *et al.* 1994, Liu *et al.* 1995, Chen *et al.* 1996) approximation is briefly summarized here for later development. In meshfree approximation, the problem domain $\bar{\Omega}$ of the mid-surface of the cylindrical panel is partitioned into a set of NP nodes $\mathbf{x}_I = (x_I, s_I)$, $I = 1, 2, \dots, NP$. The MLS/RK approximation of a dependent field variable $u(\mathbf{x})$, say $u^h(\mathbf{x})$, takes the following form:

$$u^h(\mathbf{x}) = \sum_{I=1}^{NP} \Psi_I(\mathbf{x}) d_I \quad (14)$$

where d_I is the generalized nodal coefficient and $\Psi_I(\mathbf{x})$ is the so-called MLS/RK shape function given by:

$$\begin{aligned} \Psi_I(\mathbf{x}) &= \mathbf{p}^T(\mathbf{x}_I)\mathbf{b}(\mathbf{x})\varphi_a(\mathbf{x}-\mathbf{x}_I) \\ \mathbf{p}(\mathbf{x}) &= \{p_i(\mathbf{x})\} = \{p_0(\mathbf{x}), p_1(\mathbf{x}), p_2(\mathbf{x}), \dots, p_n(\mathbf{x})\}^T \\ \mathbf{b}(\mathbf{x}) &= \{b_i(\mathbf{x})\} = \{b_0(\mathbf{x}), b_1(\mathbf{x}), b_2(\mathbf{x}), \dots, b_n(\mathbf{x})\}^T \end{aligned} \quad (15)$$

where $\mathbf{p}(\mathbf{x})$ and $\mathbf{b}(\mathbf{x})$ are the basis vector and unknown coefficient vector. $\varphi_a(\mathbf{x}-\mathbf{x}_I)$ is the kernel function centered at \mathbf{x}_I with a compact support a , which defines the smoothness and locality of the meshfree approximation. In this work a conventional cubic B-spline function (Chen *et al.* 1996) is used for the kernel function.

The unknown vector $\mathbf{b}(\mathbf{x})$ is obtained through enforcing the following n -th order reproducing conditions

$$\sum_{I=1}^{NP} \Psi_I(\mathbf{x}_I)p_i(\mathbf{x}_I) = p_i(\mathbf{x}) \quad 0 \leq i \leq n \quad (16)$$

Substituting Eq. (15) into Eq. (16) using a matrix form yields

$$\mathbf{A}(\mathbf{x})\mathbf{b}(\mathbf{x}) = \mathbf{p}(\mathbf{x}) \quad (17)$$

where $\mathbf{A}(\mathbf{x})$ is the moment matrix defined as

$$\mathbf{A}(\mathbf{x}) = \sum_{I=1}^{NP} \mathbf{p}(\mathbf{x}_I)\mathbf{p}^T(\mathbf{x}_I)\varphi_a(\mathbf{x}-\mathbf{x}_I) \quad (18)$$

After solving $\mathbf{b}(\mathbf{x}) = \mathbf{A}^{-1}(\mathbf{x})\mathbf{p}(\mathbf{x})$ from Eq. (17), the MLS/RK shape function becomes

$$\Psi_I(\mathbf{x}) = \mathbf{p}^T(\mathbf{x}_I)\mathbf{A}^{-1}(\mathbf{x})\mathbf{p}(\mathbf{x})\varphi_a(\mathbf{x}-\mathbf{x}_I) \quad (19)$$

4.2 Approximation of field variables

With the meshfree discretization, the mid-surface displacements of cylindrical panel are approximated as:

$$u^h(\mathbf{x}) = \begin{Bmatrix} u^h(\mathbf{x}) \\ v^h(\mathbf{x}) \\ w^h(\mathbf{x}) \\ \beta_x^h(\mathbf{x}) \\ \beta_\theta^h(\mathbf{x}) \end{Bmatrix} = \sum_{I=1}^{NP} \Psi_I(\mathbf{x}) \begin{Bmatrix} u_I \\ v_I \\ w_I \\ \beta_{xI} \\ \beta_{\theta I} \end{Bmatrix} \equiv \sum_{I=1}^{NP} \Psi_I(\mathbf{x}) \mathbf{d}_I \quad (20)$$

where $\mathbf{d}_I = \{u_I, v_I, w_I, \beta_{xI}, \beta_{\theta I}\}^T$. Introducing the meshfree approximation into the deformation measures then gives:

$$\boldsymbol{\varepsilon}^h(\mathbf{x}) = \begin{Bmatrix} \boldsymbol{\varepsilon}_{xx}^h \\ \boldsymbol{\varepsilon}_{\theta\theta}^h \\ \boldsymbol{\gamma}_{x\theta}^h \end{Bmatrix} = \sum_{I=1}^{NP} \mathbf{B}_I^m(\mathbf{x}) \mathbf{d}_I \quad (21)$$

$$\boldsymbol{\kappa}^h(\mathbf{x}) = \begin{Bmatrix} \boldsymbol{\kappa}_{xx}^h \\ \boldsymbol{\kappa}_{\theta\theta}^h \\ 2\boldsymbol{\kappa}_{x\theta}^h \end{Bmatrix} = \sum_{I=1}^{NP} \mathbf{B}_I^b(\mathbf{x}) \mathbf{d}_I \quad (22)$$

$$\boldsymbol{\gamma}^h(\mathbf{x}) = \begin{Bmatrix} \boldsymbol{\gamma}_{xz}^h \\ \boldsymbol{\gamma}_{\theta z}^h \end{Bmatrix} = \sum_{I=1}^{NP} \mathbf{B}_I^s(\mathbf{x}) \mathbf{d}_I \quad (23)$$

with

$$\mathbf{B}_I^m(\mathbf{x}) = \begin{bmatrix} \Psi_{I,x}(\mathbf{x}) & 0 & 0 & 0 & 0 \\ 0 & \Psi_{I,s}(\mathbf{x}) & \frac{1}{R}\Psi_I(\mathbf{x}) & 0 & 0 \\ \Psi_{I,s}(\mathbf{x}) & \Psi_{I,x}(\mathbf{x}) & 0 & 0 & 0 \end{bmatrix} \quad (24)$$

$$\mathbf{B}_I^b(\mathbf{x}) = \begin{bmatrix} 0 & 0 & 0 & \Psi_{I,x}(\mathbf{x}) & 0 \\ 0 & 0 & 0 & 0 & \Psi_{I,s}(\mathbf{x}) \\ 0 & 0 & 0 & \Psi_{I,s}(\mathbf{x}) & \Psi_{I,x}(\mathbf{x}) \end{bmatrix} \quad (25)$$

$$\mathbf{B}_I^s(\mathbf{x}) = \begin{bmatrix} 0 & 0 & \Psi_{I,x}(\mathbf{x}) & -\Psi_I(\mathbf{x}) & 0 \\ 0 & -\frac{1}{R}\Psi_I(\mathbf{x}) & \Psi_{I,s}(\mathbf{x}) & 0 & -\Psi_I(\mathbf{x}) \end{bmatrix} \quad (26)$$

4.3 Representation of pure bending mode

To construct a locking free numerical scheme, the meshfree approximations are expected to reproduce the Kirchhoff mode (pure bending) discussed in Eq. (11), i.e., meet the requirement of KMRC. According to Eq. (11), a pure bending nodal coefficient vector takes the form of:

$$\mathbf{d}_I^b = \begin{Bmatrix} 0 \\ cR^2(\sin \theta_I - \theta_I) \\ cR^2(1 - \cos \theta_I) \\ 0 \\ cR \theta_I \end{Bmatrix} \quad (27)$$

Thus the discrete counterparts of Eq. (12) are:

$$\left\{ \begin{array}{l} \sum_{I=1}^{NP} \mathbf{B}_I^m \mathbf{d}_I^b = 0 \\ \sum_{I=1}^{NP} \mathbf{B}_I^b \mathbf{d}_I^b = 0 \\ \sum_{I=1}^{NP} \mathbf{B}_I^b \mathbf{d}_I^b = \begin{Bmatrix} 0 \\ c \\ 0 \end{Bmatrix} = \text{constant} \end{array} \right. \quad (28)$$

or

$$\left\{ \begin{array}{l} \sum_{I=1}^{NP} \Psi_I = 1 \\ \sum_{I=1}^{NP} \Psi_{I,s} s_I = s; \sum_{I=1}^{NP} \Psi_{I,s} s_I = 1 \\ \sum_{I=1}^{NP} [\Psi_{I,s} R \cos \theta_I + \Psi_I \sin \theta_I] = 0 \\ \sum_{I=1}^{NP} [\Psi_{I,s} R \sin \theta_I + \Psi_I \cos \theta_I] = 0 \end{array} \right. \quad (29)$$

It is straightforward to show that the reproducing properties of Eq. (29) can be satisfied by taking the following MLS/RK basis:

$$\mathbf{p}(\mathbf{x}) = \{1 \ x \ s \ x^2 \ x s \ \sin(s/R) \ \cos(s/R)\}^T \quad (30)$$

Not that the basis vector $\mathbf{p}(\mathbf{x})$ includes the enhanced bending terms, $\sin(s/R)$ and $\cos(s/R)$.

5. Integration constraint, smoothed curvature and SCNI formulation

5.1 Integration constraint and smoothed curvature

Satisfaction of KMRC by the MLS/RK approximation is just one requirement to yield a pure bending solution using the Galerkin variational formulation, moreover, the integration of the variational form also needs to fulfill the integration constraint (Chen *et al.* 2001, Wang and Chen 2004). The integration constraint can be obtained through imposing the pure bending mode on the weak form, as leads to:

$$\int_{\Omega} \delta \boldsymbol{\kappa}^{hT} \mathbf{D}^b \boldsymbol{\kappa}^h d\Omega = - \int_{\Gamma} \delta \boldsymbol{\beta}^{hT} \bar{\mathbf{M}} d\Gamma \quad (31)$$

where $\bar{\mathbf{M}}$ is the prescribed moment due to a pure bending mode. Without going into the details,

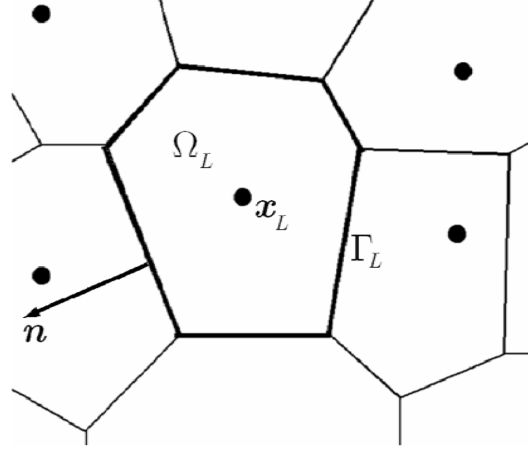


Fig. 2 Nodal representative domain

similar argument as in Wang and Chen (2004) leads to the following integration constraint:

$$\int_{\Omega}^{INT} \mathbf{B}_I^{bT} d\Omega = \int_{\Gamma}^{BINT} \mathbf{G}_I^T d\Gamma \quad (32)$$

where the superscripts *INT* and *BINT* denote numerical domain and boundary integrations, respectively. \mathbf{G}_I is given by

$$\mathbf{G}_I = \begin{bmatrix} 0 & 0 & 0 & \Psi_I n_x & 0 \\ 0 & 0 & 0 & 0 & \Psi_I n_s \\ 0 & 0 & 0 & \Psi_I n_s & \Psi_I n_x \end{bmatrix} \quad (33)$$

The SCNI method has been developed to fulfill the integration constraint and thus can achieve bending exactness under the Galerkin variational framework (Chen *et al.* 2001, Wang and Chen 2004). In this approach, a smoothed nodal curvature as shown below is employed with the nodal integration:

$$\begin{aligned} \tilde{\kappa}_{ij}(\mathbf{x}_L) &= \frac{1}{2A_L} \int_{\Omega_L} (\beta_{i,j} + \beta_{j,i}) d\Omega \\ &= \frac{1}{2A_L} \int_{\Gamma_L} (\beta_i n_j + \beta_j n_i) d\Gamma \quad i, j = \{x, s\} \end{aligned} \quad (34)$$

where Ω_L and Γ_L are the nodal representative domain and its boundary for node $\mathbf{x}_L = (x_L, s_L)$ as shown in Fig. 2. A_L denotes the area of Ω_L .

Thus the smoothed nodal curvature has the form:

$$\tilde{\kappa}^h(\mathbf{x}_K) = \begin{Bmatrix} \tilde{\kappa}_{xx}^h(\mathbf{x}_K) \\ \tilde{\kappa}_{\theta\theta}^h(\mathbf{x}_K) \\ 2\tilde{\kappa}_{x\theta}^h(\mathbf{x}_K) \end{Bmatrix} = \sum_{I=1}^{NP} \tilde{\mathbf{B}}_I^b(\mathbf{x}_K) \mathbf{d}_I \quad (35)$$

where

$$\tilde{\mathbf{B}}_I^b(\mathbf{x}_L) = \begin{bmatrix} 0 & 0 & 0 & \tilde{\Psi}_{I,x}(\mathbf{x}_L) & 0 \\ 0 & 0 & 0 & 0 & \tilde{\Psi}_{I,s}(\mathbf{x}_L) \\ 0 & 0 & 0 & \tilde{\Psi}_{I,s}(\mathbf{x}_L) & \tilde{\Psi}_{I,x}(\mathbf{x}_L) \end{bmatrix} \quad (36)$$

with $\tilde{\Psi}_{I,i}(\mathbf{x}_L)$ being the smoothed nodal gradient of shape function given by:

$$\tilde{\Psi}_{I,i}(\mathbf{x}_L) = \frac{1}{A_L} \int_{\Gamma_L} \tilde{\Psi}_I(\mathbf{x}) n_i(\mathbf{x}) d\Gamma, \quad i = \{x, s\} \quad (37)$$

5.2 Properties of smoothed nodal gradient

Here we show that the smoothed gradient defined in Eq. (37) preserves the following desired reproducing properties which hold for the standard shape function gradient:

$$\begin{aligned} \sum_{I=1}^{NP} \tilde{\Psi}_{I,i}(\mathbf{x}_L) &= \sum_{I=1}^{NP} \left(\frac{1}{A_L} \int_{\Gamma_L} \Psi_I n_i d\Gamma \right) = \frac{1}{A_L} \int_{\Gamma_L} \left(\sum_{I=1}^{NP} \Psi_I \right) n_i d\Gamma \\ &= \frac{1}{A_L} \int_{\Gamma_L} 1 \times n_i d\Gamma = \frac{1}{A_L} \int_{\Omega_L} 1_{,i} d\Omega = 0 \quad i = \{x, s\} \end{aligned} \quad (38)$$

$$\begin{aligned} \sum_{I=1}^{NP} \tilde{\Psi}_{I,i}(\mathbf{x}_L) x_{jI} &= \sum_{I=1}^{NP} \left(\frac{1}{A_L} \int_{\Gamma_L} \Psi_I x_{jI} n_i d\Gamma \right) = \frac{1}{A_L} \int_{\Gamma_L} \left(\sum_{I=1}^{NP} \Psi_I x_{jI} \right) n_i d\Gamma \\ &= \frac{1}{A_L} \int_{\Gamma_L} x_j \times n_i d\Gamma = \frac{1}{A_L} \int_{\Omega_L} \delta_{ij} d\Omega = \delta_{ij} \quad i = \{x, s\} \end{aligned} \quad (39)$$

where use is made of the reproducing conditions of Eq. (16). Also we use the notations $x_1 = x$, $x_2 = s$.

Thus in summary we have

$$\begin{cases} \sum_{I=1}^{NP} \tilde{\Psi}_{I,i}(\mathbf{x}_L) = 0 \\ \sum_{I=1}^{NP} \tilde{\Psi}_{I,x}(\mathbf{x}_L) x_I = 1, \sum_{I=1}^{NP} \tilde{\Psi}_{I,s}(\mathbf{x}_L) x_I = 0 \quad L = 1, 2, \dots, NP \\ \sum_{I=1}^{NP} \tilde{\Psi}_{I,x}(\mathbf{x}_L) s_I = 0, \sum_{I=1}^{NP} \tilde{\Psi}_{I,s}(\mathbf{x}_L) s_I = 1 \end{cases} \quad (40)$$

These properties are necessary for the meshfree approximation to produce a constant strain field and note that the first equation of (40) is widely referred as the partition of nullity.

5.3 SCNI discretized meshfree equations

In the SCNI approach, the assumed strain method (Simo and Hughes 1985) is employed and the smooth nodal curvature of Eq. (35) is employed in the nodally integrated variational form of Eq. (10), which yields $\delta \Pi(\mathbf{u}^h, \tilde{\mathbf{K}}^h)(\mathbf{x}_L) = 0$. Then the standard variational arguments lead to the following discretized equilibrium equations:

$$\mathbf{K}d = (\mathbf{K}^m + \mathbf{K}^b + \mathbf{K}^s)d = \mathbf{f} \quad (41)$$

where the components of \mathbf{K}^b , \mathbf{K}^m , \mathbf{K}^s and \mathbf{f} are give by:

$$\left\{ \begin{array}{l} \mathbf{K}_{IJ}^m = \sum_{L=1}^{NP} \mathbf{B}_I^{mT}(\mathbf{x}_L) \mathbf{D}^m \mathbf{B}_J^m(\mathbf{x}_L) A_L \\ \mathbf{K}_{IJ}^b = \sum_{L=1}^{NP} \tilde{\mathbf{B}}_I^{bT}(\mathbf{x}_L) \mathbf{D}^b \tilde{\mathbf{B}}_J^b(\mathbf{x}_L) A_L \\ \mathbf{K}_{IJ}^s = \sum_{L=1}^{NP} \mathbf{B}_I^{sT}(\mathbf{x}_L) \mathbf{D}^s \mathbf{B}_J^s(\mathbf{x}_L) A_L \end{array} \right. \quad (42)$$

$$\mathbf{f}_I = \sum_{L=1}^{NP} \Psi_I(\mathbf{x}_L) \left\{ \begin{array}{l} p_x(\mathbf{x}_L) \\ p_x(\mathbf{x}_L) \\ q(\mathbf{x}_L) \\ m_x(\mathbf{x}_L) \\ m_s(\mathbf{x}_L) \end{array} \right\} A_K + \sum_{K=1}^{NP} \Psi_I(\bar{\mathbf{x}}_K) \left\{ \begin{array}{l} \bar{N}_x(\bar{\mathbf{x}}_K) \\ \bar{N}_\theta(\bar{\mathbf{x}}_K) \\ \bar{Q}_z(\bar{\mathbf{x}}_K) \\ -\bar{M}_x(\bar{\mathbf{x}}_K) \\ -\bar{M}_s(\bar{\mathbf{x}}_K) \end{array} \right\} \bar{w}_K \quad (43)$$

with NB and \bar{w}_K being the number of boundary integration points and corresponding weight of integration.

6. Numerical examples

6.1 Scordelis-Lo roof

The Scordelis-Lo roof subjected to gravity load is one widely recognized problem to test the effectiveness of numerical shell formulation. The geometry, material and loading information is listed in Fig. 3, where the roof is longitudinally supported by two rigid end diaphragms and the other two edges of the roof are free. The reference solution for the deflection at the mid-span of the free edge (C) is 0.3024 (MacNeal and Harder1985). Taking advantage of the two directional symmetries, only a quarter of the structure is discretized. The various meshfree discretizations employed here are shown in Fig. 4. A normalized support size of 3.5 is taken through this analysis. In Fig. 5, the normalized vertical displacement of point C obtained by the present method is

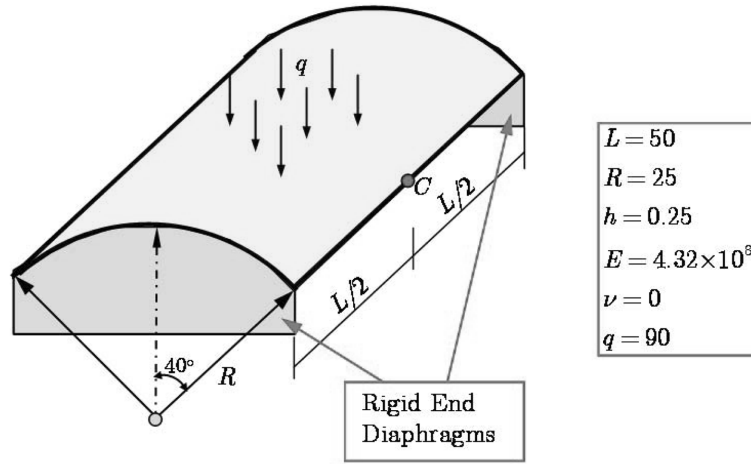


Fig. 3 Problem description of Scordelis-Lo roof

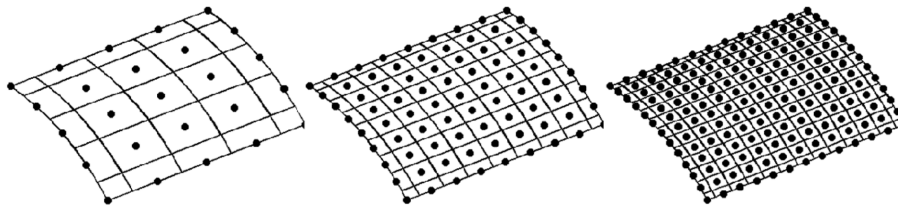


Fig. 4 Meshfree discretizations for Scordelis-Lo roof

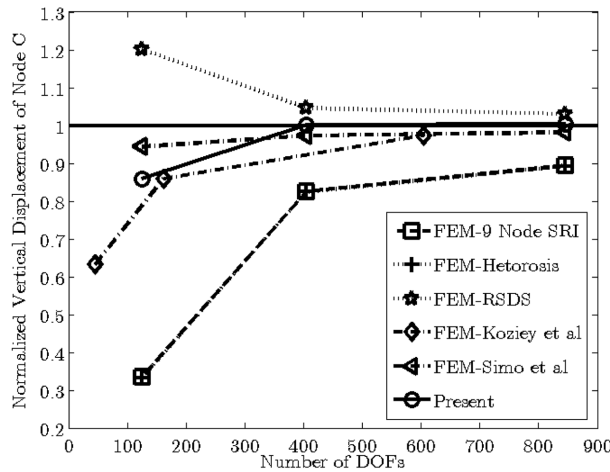


Fig. 5 Comparison of normalized vertical displacement of node C for the problem of Scordelis-Lo roof

compared to some well-known FEM results (9 Node SRI (Liu *et al.* 1986), RSDS (Liu *et al.* 1986), Heterosis (Liu *et al.* 1986), (Koziey and Mirza 1997), (Simo *et al.* 1989)). The numerical results evince that the proposed approach performs very well compared with these published finite element solutions.

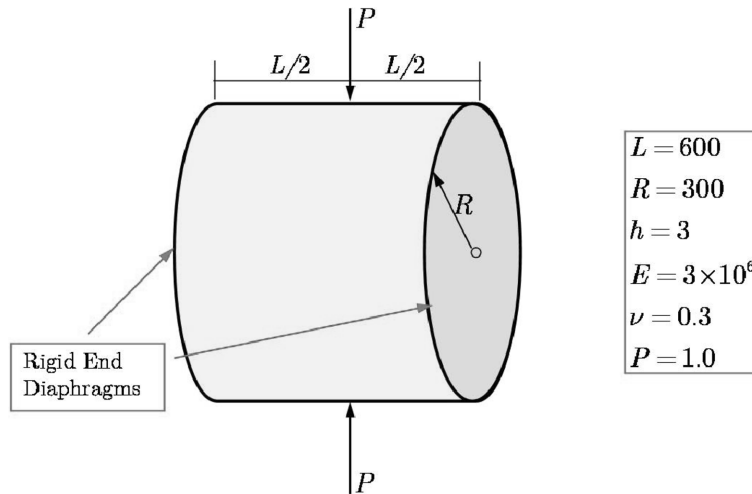


Fig. 6 Problem description of pinched cylinder with rigid end diaphragms

6.2 Pinched cylinder with rigid end diaphragms

Another benchmark example we consider here is the classical problem of pinched cylinder with rigid diaphragms at the two ends. The cylinder is subjected to a pair of equal and opposite point loads at its mid-span. The problem statement is shown in Fig. 6. This problem is frequently employed to comprehensively assess the capability of a numerical method for representing the bending, shear, and membrane modes. The reference solution of the deflection underneath the concentrated force is 1.82488×10^{-5} (Simo *et al.* 1989). Only one-eighth of the cylinder is modeled by invoking the three-fold symmetry of this problem. Fig. 7 lists the different meshfree discretizations employed in this study in which a normalized support size of 4.0 is used. In Fig. 8, the comparison of normalized deflection under the point force is given between the proposed solution and other solutions using the FEM methods by (Simo *et al.* 1989), (Koziey and Mirza 1977), 9 Node SRI (Simo *et al.* 1989), the EFG shear deformable shell formulation by (Noguchi *et al.* 2000), and the constrained reproducing kernel global meshfree shell approach (CRK-Global shell) by (Chen and Wang 2004, Chen and Wang 2006). The numerical results show that the solution of current method compares favorably to those obtained from the finite element and meshfree solutions we just mentioned.

7. Conclusions

An efficient Galerkin meshfree approach was presented for the analysis of shear deformable cylindrical panels. The present formulation is featured by an enhanced meshfree basis function for accuracy and the accelerated stabilized conforming nodal integration for efficiency and stability. The enhanced basis function was deduced from the Kirchhoff mode reproducing condition of the pure bending mode constructed based upon its counterpart of the curved beam. Thus the approximated meshfree solution using the enhanced basis does not yield parasitic shear and membrane deformations in representing the

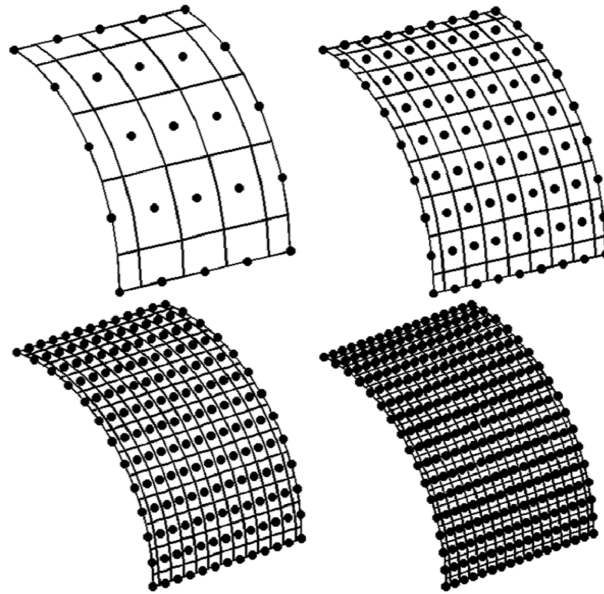


Fig. 7 Meshfree discretizations for pinched cylinder with end diaphragms

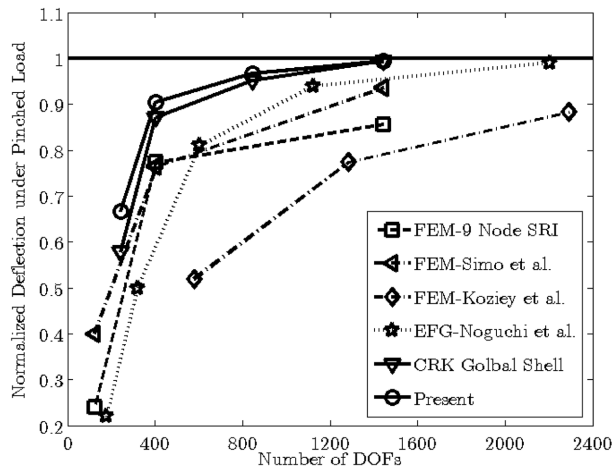


Fig. 8 Comparison of normalized deflection underneath the point load for the problem of pinched cylinder with rigid end diaphragms

pure bending mode. To fulfill the integration constraint of Galerkin weak form associated with the bending exactness, a curvature smoothing operation at nodal points was performed. It was proved the smoothed nodal gradient resulting from the curvature smoothing operation inherits some desired characteristics, i.e., the partition of nullity and reproduction of a constant strain field, which hold for the conventional differentiation based nodal gradient of meshfree shape function. Very favorable numerical performance of the present formulation was observed from two benchmark examples, the Scordelis-Lo Roof problem and the problem of pinched cylinder with rigid end diaphragms.

Acknowledgements

The support of this work by the National Natural Science Foundation of China under grant number 10602049 and the Program for New Century Excellent Talents in Fujian Province University of China is gratefully acknowledged.

References

- Lancaster, P. and Salkauskas, K. (1981), "Surfaces generated by moving least squares methods", *Mathematics of Computation*, **37**, 141-158.
- Belytschko, T., Lu, Y.Y. and Gu, L. (1994), "Element-free Galerkin methods", *Int. J. Numer. Methods Eng.*, **37**, 229-256.
- Liu, W. K., Jun, S. and Zhang, Y.F. (1995), "Reproducing kernel particle methods", *Int. J. Numer. Methods Fluids*, **20**, 1081-1106.
- Chen, J.S., Pan, C., Wu, C.T. and Liu, W.K. (1996), "Reproducing kernel particle methods for large deformation analysis of nonlinear structures", *Comput. Methods Appl. Mech. Eng.*, **139**, 195-227.
- Krysl, P. and Belytschko, T. (1996), "Analysis of thin shells by the element-free Galerkin method", *Int. J. Solids Struct.*, **33**, 3057-3080.
- Li, S., Hao W. and Liu, W.K. (2000), "Numerical simulations of large deformation of thin shell structures using meshfree method", *Comput. Mech.*, **25**, 102-116.
- Li, S. and Liu, W.K. (2004), *Meshfree Particle Methods*, Springer, Germany.
- Hallquist, J.O. (2003), "Current and future developments of LS-DYNA II", *Proceeding of 4th European LS-DYNA Users Conference*, ULM, Germany, May.
- Beissel, S. and Belytschko, T. (1996), "Nodal integration of the element-free Galerkin method", *Comput. Methods Appl. Mech. Eng.*, **139**, 49-74.
- Dyka, C.T. and Ingel, R.P. (1995), "An approach for tensile instability in smoothed particle hydrodynamics", *Comput. Struct.*, **57**, 573-580.
- Randles, P.W. and Libersky, L.D. (2000), "Normalized SPH with stress points", *Int. J. Numer. Methods Eng.*, **48**, 1445-1462.
- Rabczuk, T., Belytschko, T. and Xiao, S.P. (2004), "Stable particle methods based on Lagrangian kernels", *Comput. Methods Appl. Mech. Eng.*, **193**, 1035-1063.
- Chen, J.S., Wu, C.T., Yoon, S. and You, Y. (2001), "A stabilized conforming nodal integration for Galerkin meshfree methods", *Int. J. Numer. Methods Eng.*, **50**, 435-466.
- Chen, J.S., Yoon, S. and Wu, C.T. (2002), "Nonlinear version of stabilized conforming nodal integration for Galerkin meshfree methods", *Int. J. Numer. Methods Eng.*, **53**, 2587-2615.
- Chen, J.S., Wang, D. and Dong, S.B. (2004), "An extended meshfree method for boundary value problems", *Comput. Methods Appl. Mech. Eng.*, **193**, 1085-1103.
- Wang, D. and Chen, J.S. (2004), "Locking-free stabilized conforming nodal integration for meshfree Mindlin-Reissner plate formulation", *Comput. Methods Appl. Mech. Eng.*, **193**, 1065-1083.
- Wang, D., Dong, S.B. and Chen, J.S. (2006), "Extended meshfree analysis of transverse and inplane loading of a laminated anisotropic plate of general planform geometry", *Int. J. Solids Struct.*, **43**, 144-171.
- Wang, D. and Chen, J.S. (2004), "Constrained reproducing kernel formulation for shear deformable shells", *Proceeding of the 6th World Congress on Computational Mechanics*, Beijing, China, September.
- Wang, D. and Chen, J.S. (2006), "A locking-free meshfree curved beam formulation with the stabilized conforming nodal integration", *Comput. Mech.*, **39**, 83-90.
- Chen, J.S. and Wang, D. (2006), "A constrained reproducing kernel particle formulation for shear deformable shell in Cartesian coordinates", *Int. J. Numer. Methods Eng.*, **68**, 151-172.
- Wang, D. (2006), "A stabilized conforming integration procedure for Galerkin meshfree analysis of thin beam and plate", *Proceeding of the 10th Enhancement and Promotion of Computational Methods in Engineering and Science (EPMESC-X)*, Sanya, China, August.
- Wang, D. and Chen, J.S. (2008), "A Hermite reproducing kernel approximation for thin plate analysis with sub-

- domain stabilized conforming integration”, *Int. J. Numer. Methods Eng.*, **74**, 368-390.
- Timoshenko, S.P. and Woinowsky-Krieger, S. (1959), *Theory of Plates and Shells* (2nd edn), McGraw-Hill, New York.
- Simo, J.C. and Hughes, T.J.R. (1985), “On the variational foundation of assumed strain method”, *J. Appl. Mech.*, **53**, 51-54.
- MacNeal, R.H. and Harder, R.L. (1985), “A proposed standard set of problems to test finite element accuracy”, *Finite Elements in Analysis and Design*, **1**, 3-20.
- Liu, W.K., Law S.E., Lam, D. and Belytschko, T. (1986), “Resultant stress degenerated shell elements”, *Comput. Methods Appl. Mech. Eng.*, **55**, 259-300.
- Koziey, B.L. and Mirza, F.A. (1997), “Consistent thick shell element”, *Comput. Struct.*, **65**, 531-549.
- Simo, J.C., Fox, D.D. and Rifai M.S. (1989), “On a stress resultant geometrical exact shell model. Part II: the linear theory; computational aspects”, *Comput. Methods Appl. Mech. Eng.*, **73**, 53-92.
- Noguchi, H., Hawashima, T. and Miyamura, T. (2000), “Element free analysis of shell and spatial structures”, *Int. J. Numer. Methods Eng.*, **47**, 1215-1240.